BASIC SCIENCE

Nanomedicine: Nanotechnology, Biology, and Medicine
20 (2019) 101983

Original Article

nanomedjournal.com

The phenotype of target pancreatic cancer cells influences cell death by magnetic hyperthermia with nanoparticles carrying gemicitabine and the pseudo-peptide NucAnt

Mourad Sanhaji, PhD[a], Julia Göring[a], Pierre Couleaud, PhD[b,c], Antonio Aires, PhD[b,c], Aitziber L. Cortajarena, PhD[b,c], José Courty, PhD[d], Adriele Prina-Mello, PhD[e], Marcus Stapf, PhD[a], Robert Ludwig, PhD[a], Yuri Volkov, PhD[e], Alfonso Latorre, PhD[b,c], Álvaro Somoza, PhD[b,c], Rodolfo Miranda, PhD[b,c], Ingrid Hilger, PhD[a,*]

[a]*Institute for Diagnostic and Interventional Radiology, Jena University Hospital–Friedrich Schiller University Jena, Jena, Germany*
[b]*Instituto Madrileño de Estudios Avanzados en Nanociencia (IMDEA Nanociencia), Campus Universitario de Cantoblanco, Madrid, Spain*
[c]*Unidad Asociada de Nanobiotecnología CNB-CSIC & IMDEA Nanociencia, Campus Universitario de Cantoblanco, Madrid, Spain*
[d]*Laboratoire CRRET, Université Paris EST Créteil, 61 Avenue du Général de Gaulle, Créteil, France*
[e]*Nanomedicine and Molecular Imaging group, Trinity Translational Medicine Institute, Trinity College Dublin, Dublin, Ireland*

Revised 17 December 2018

Abstract

In this paper we show that conjugation of magnetic nanoparticles (MNPs) with Gemcitabine and/or NucAnt (N6L) fostered their internalization into pancreatic tumor cells and that the coupling procedure did not alter the cytotoxic potential of the drugs. By treating tumor cells (BxPC3 and PANC-1) with the conjugated MNPs and magnetic hyperthermia (43 °C, 60 min), cell death was observed. The two pancreatic tumor cell lines showed different reactions against the combined therapy according to their intrinsic sensitivity against Gemcitabine (cell death, ROS production, ability to activate ERK 1/2 and JNK). Finally, tumors (*e.g.* 3 mL) could be effectively treated by using almost 4.2×10^5 times lower Gemcitabine doses compared to conventional therapies. Our data show that this combinatorial therapy might well play an important role in certain cell phenotypes with low readiness of ROS production. This would be of great significance in distinctly optimizing local pancreatic tumor treatments.
© 2019 The Authors. Published by Elsevier Inc. This is an open access article under the CC BY-NC-ND license (http://creativecommons.org/licenses/by-nc-nd/4.0/).

Key words: Magnetic hyperthermia; Magnetic nanoparticles (MNP); Gemcitabine (Gem); NucAnt (N6L); Pancreatic cancer; Mouse model

Pancreatic carcinoma is among the most harmful cancers, which are associated with poor prognosis. Despite very aggressive surgical and chemotherapeutical interventions, this cancer entity still causes one of the highest cancer associated deaths in Europe and in North America.[1,2]

Owing to the high mortalities, intensive research is being undertaken to find more effective therapy options.[3] One of them is magnetic hyperthermia, which is sought to be a promising tool in the field of anti-cancer therapy.[4,5] It is based on the heat generated by magnetic nanoparticles (MNPs), when these are later subjected to an alternating magnetic field. Besides the role in generating local heat inside tumor tissue, iron oxide based MNPs have been approved as a contrast agent for MRI and suggested for photothermal therapy approaches.[6] More importantly, the surface of MNPs can be used as a platform for multivalent drug conjugation and delivery.[7–9] Several *in vivo*

Acknowledgments: The described work was carried out within the project "Multifunctional Nanoparticles for the Selective Detection and Treatment of Cancer" (Multifun), funded by the European Commission (No. 262943) and in parts by Horizon 2020 (NoCanTher EC 685795). We thank Dr. Vijay Patel and Liquids Research Ltd. (Mentec, Deiniol Road, Bangor, Gwynedd, North Wales, UK,) for the supply of MF66. We gratefully acknowledge Susann Burgold for technical assistance in carrying out *in vivo* experiments and Kieran Crosbie-Staunton in carrying out the *in vitro* toxicity experiments.

*Corresponding author at: Institute for Diagnostic and Interventional Radiology, Jena University Hospital–Friedrich Schiller University Jena, Jena. Tel.: +49 3641 9325921; fax: +49 3641 9325922.

E-mail address: ingrid.hilger@med.uni-jena.de. (I. Hilger).

https://doi.org/10.1016/j.nano.2018.12.019
1549-9634/© 2019 The Authors. Published by Elsevier Inc. This is an open access article under the CC BY-NC-ND license (http://creativecommons.org/licenses/by-nc-nd/4.0/).

Please cite this article as: Sanhaji M, et al, The phenotype of target pancreatic cancer cells influences cell death by magnetic hyperthermia with nanoparticles carrying gemicitabine and the pseudo-peptide NucAnt. *Nanomedicine: NBM* 2019;20:101983, https://doi.org/10.1016/j.nano.2018.12.019

and *in vitro* studies reported the efficiency of magnetic hyperthermia in triggering the release of the chemotherapeutics form the MNP drug carrier[10,11] as well as its synergistic effect when combined with different types of chemotherapeutics.[5,12]

A standard care strategy for patients with pancreatic tumors is the chemotherapeutic agent gemcitabine (Gem). It is a cytidine analog that is incorporated into DNA during replication causing cell cycle arrest and ultimately leading to apoptosis.[13,14] It has been approved as first line treatment of non-small lung, bladder, breast and pancreatic cancers.[15] Although Gem-based chemotherapy provides clinical advantages for patients, important amount of studies reported the emergence of resistances.[16–18] Commonly known side effects of Gem after systemic application include, fever, nausea, low blood counts *etc.*

In contrast a high tolerability and effectivity in pancreatic cancer treatment can be achieved by coupling the drug to magnetic nanoparticles in order to exploit the synergistic effects of magnetic hyperthermia and chemotherapy. However, there are still some challenges facing the use of chemotherapeutic loaded MNPs, such as the reduced accumulation of these nanoparticles in the tumor tissues after systemic injection.[19] Therefore, the intratumoral injection of the magnetic material is the method of choice for clinical translation. In order to foster the intracellular accumulation of MNPs deposited in the tumors and the anticancer activity during therapy, the consideration of the pseudo-peptide N6L is favorable[20] It recognizes specifically nucleolin,[21] which is a protein overexpressed on the surface of cancer cells, as well as nucleophosmin. This permits its entry into the nucleus, which mediates the induction of apoptosis.[20,22,23]

In the present work, using *in vitro* investigations and an *in vivo* pancreatic mouse model, we sought to investigate to which extent magnetic nanoparticles conjugated with Gem and N6L do exert a synergistic effect on tumor phenotype when subjected to an alternating magnetic field to deliver magnetically induced heating. In this context we asked the following questions: 1) What is the specific absorption rate of the nanoparticles with consideration of their immobilization in tumor structures? 2) Is there a combined effect between the conjugated MNPs and magnetic hyperthermia on the phenotype of pancreatic tumor cells? 3) If yes, to which extent is the combined effect able to inhibit tumor cell growth by inducing an S-phase cell cycle arrest and cell death (apoptosis and non-apoptotic cell death)? 4) To what degree can the combined effect be attributed to the onset of cellular stress mechanisms (*e.g.* ROS production, activation of JNK kinase pathways)? 5) Is the multifactorial (Gem and/or N6L and hyperthermia) therapy modality compatible to living animals?

Methods

Magnetic nanoparticle synthesis

Magnetic nanoparticles (MNPs) were made up of an iron oxide core and a dimercapto-succnic acid (DMSA) coating.[24] For experimental sakes, these nanoparticles were called MF66. The hydrodynamic diameter of MF66 was assessed using dynamic light scattering (DLS) and Nanoparticle Tracking Analysis (NTA).

Conjugation of DMSA-MNP

MF66 were covalently bi-conjugated with both gemcitabine (Gem)[13] or the pseudo-peptide NucAnt (N6L) as described previously.[25] Finally, the final concentration of drugs conjugated to MNPs was 5 μmol N6L/g Fe and 12 μmol GEM/g Fe.

Specific absorption rate of MNP

The specific absorption rate (SAR) of the different MNP formulations was assessed as described before.[24,26]

Cells, culture, and MNP exposure conditions

The BxPC-3 and PANC-1 cell lines were selected because of their different sensitivity against Gem (BxPC-3: high, PANC-1: low[27]) and different ROS responsiveness after magnetic hyperthermia (BxPC-3: high, PANC-1: low[28]). Both cell lines (ATCC) were cultured in RPMI 1640 medium complemented with 10% fetal bovine serum (Gibco ®). Cells were kept at 37 °C and a humidified atmosphere containing 5% CO_2. For experimentation, cells were incubated with the nanoparticles for 24 h and subjected or not (controls, MNP groups) to magnetic hyperthermia (43 °C, 60 min, alternating magnetic field (AMF); denoted as MNP + AMF groups).

Quantification of MNP cellular uptake using atomic absorption spectrometry (AAS)

Cells were incubated with the different MNP formulations for 24 h. Quantification of intracellular iron content was performed as described previously.[24]

Cell growth assay

Cells were grown on cell culture flasks and either incubated with the different MNP formulations (concentration of 100 μg Fe / ml, group 1) or additionally subjected to an alternating magnetic (60 min, 24 h after MNPs incubation, group 2). At 24 or 48 h later, the cell growth was determined.[29] Fluorescence (λ_{exc} = 530-560 nm, λ_{em} = 590 nm) was normalized to the one of the untreated cells. The experiment was carried out at least 3 times.

Cytotoxicity evaluation of conjugated MNP by High Content Screening and Analysis (HCSA)

HCSA was carried out on incubated cells to evaluate cell count reduction, membrane permeability, lysosomal mass /pH variation as previously described.[30–32] Cytotoxicity exposure and analysis followed the same protocol as previously published.[30] Bioinformatics was carried out to identify cytotoxicity behavior for dose-dependent exposures, as previously described.[31,32]

2D colony formation assay

Evaluation of 2D survival after treatment of the cells was performed as described in a previous publication.[33]

Analysis of cell cycle distribution and apoptosis using flow cytometry

Cells were seeded and incubated with MNPs (see above). 24 and 48 h post hyperthermia, cells were collected, washed and prepared as described elsewhere.[34] The data were analyzed with the CELLQUEST Pro software (BD Biosciences, Heidelberg, Germany).

Analysis of cell death by Annexin V/ 7-Amino-Actinomycin (7-AAD) binding by flow cytometry

Cells were harvested, washed with cold PBS, and stained with Annexin V-FITC / 7AAD according to manufacturer's protocol.[35]

Measurement of intracellular reactive oxygen species (ROS) level

The generation of cellular ROS was monitored by measuring the oxidation of dichloro-dihydro-fluorescein diacetate (DCFH-DA) to 2′,7′-dichlorofluorescein (DCF). Upon MNPs + AMF and MNP treatments, cells were washed with PBS followed by addition of 10 μM working solution of DCFH-DA (Sigma, Darmstadt, Germany) at 37 °C for 1 h. Lastly, cells were washed with PBS and the fluorescence was assessed spectroscopically (at λ_{exc} = 485 nm, λ_{em} = 535 nm).

Western blot analysis, active caspase 3/7, and active caspase 8 measurements

Cell lysis was performed with RIPA buffer and protease inhibitor cocktail complete (Roche). Western blot analysis was performed as previously described.[36] Mouse antibodies against p53, Bcl-2, Bax, rabbit antibodies against, Cyclin A, were purchased from Santa Cruz biotechnology. Mouse antibodies against cleaved-PARP, δ-H2AX, rabbit antibodies against JNK, p-JNK, Erk, p-Erk, p-C-Jun, cleaved Caspase 3, p21 were obtained from Cell Signaling. Measurement of the activities of caspase 3/7 and caspase 8 was performed using Caspase-Glo® 3/7 and Caspase-Glo® 8 Assays (Promega, Mannheim, Germany) according to manufacturer's instructions.

In vivo hyperthermia experiments in BxPC-3 mouse models

The experiments were carried out in accordance with international guidelines on the ethical use of animals and were approved by the regional animal care committee (Thüringer Landesamt für Verbraucherschutz, Bad Langensalza, Germany). Animals were humanely cared for during the whole experimentation period. Animals were maintained under artificial day–night cycles (12 h light–dark cycles; 23 °C room temperature, 30%-60% environment humidity) and received food and water *ad libitum*. **A**thymic nude mice were subcutaneously injected with 2×10^6 BxPC-3 cells. Tumors of a volume between 100 and 250 mm^3, were injected with 0.25 mg Fe, 3 nmol Gem, and/or 1.25 nmol N6L per 100 mm^3 of the different MNP formulations (12 μmol Gem and 5 μmol N6L per g Fe). Two *in vivo* hyperthermia treatments, at day 0 and day 7 were performed. Mice were subjected to an alternating magnetic field for 60 min to temperatures around 43 °C. Fiber optic temperature sensors (Optocon, Dresden, Germany) monitored the temperature at the tumor surface and the rectal temperatures of the mice during the whole experimental procedure. The tumor volumes of the different treatment groups were compared to those of the control group that only received ddH_2O since the MNP formulations were suspended in water. All animal handling was performed under anesthesia.

Histology of Ki67 in BxPC-3 tumors after treatment with MNP-N6LGem

Tumors were fixed in formaldehyde and embedded in paraffin. Tissue slices were blocked with avidin and biotin, incubated with the primary antibody for Ki67 (Abcam, Berlin, Germany) secondary one (goat anti-rabbit IgG (H + L)-biotin (Dianova, Hamburg, Germany). Antigen detection of Ki67 was achieved using streptavidin AP (Biozol, Eching, Germany) and a chromogen (Dako, Glostrup, Germany). Slices were counterstained with hematoxylin (Sigma-Aldrich, Karlsruhe). Semi-quantitative analysis of Ki67-staining was performed with the software "cellSens Dimension" from Olympus (Düsseldorf, Germany). Hereto, 400 cells were counted per hotspot at 20-fold magnification and were assigned to either to the Ki67-positive or Ki67-negative group.

Statistical analysis and calculations

Student's *t* test (two tailed and paired) was used to evaluate the significance of differences between the treatment groups within the experiments. Difference was considered as statistically significant when $P < 0.05$. For comparison of Gemcitabine doses in oncological therapies *vs.* intratumorally applied ones see supplemental text.

Results

MF66 MNP formulations show a high heating potential and a good cellular uptake

The MF66 MNPs were successfully conjugated either with the chemotherapeutic gemcitabine (Gem) or the pseudo-peptide NucAnt (N6L), as well as with both. The conjugation of MF66 DMSA-MNPs increased their hydrodynamic diameter (Figure 1, *A*). Due to the positive charges of N6L, we obtained a positive zeta potential for MF66-N6L and the bi-conjugated MF66-N6LGem (Figure 1, *C*). The investigated MNPs showed very high SAR value as suspension in water. Under different immobilization conditions (in 1% agarose or 10% PVA), we observed a SAR reduction in all MNP formulations. The strongest reduction was observed in 10% PVA, where the SAR values were found to be reduced by 50% in all MNP formulations compared to the situation before MNPs immobilization (Figure 1, *D*). All MNP formulations were internalized by BxPC-3 cells but at different extents. Interestingly, conjugated MNPs showed the best uptake compared to the non-conjugated MF66 (Figure 1, *E*).

Cytotoxicity of conjugated MNPs

Multi-parametric analysis showed that MNP-concentrations up to 100 μg Fe/mL did not trigger MNP-induced cytotoxicity, as from previously reported work for breast cancer cell lines.[30]

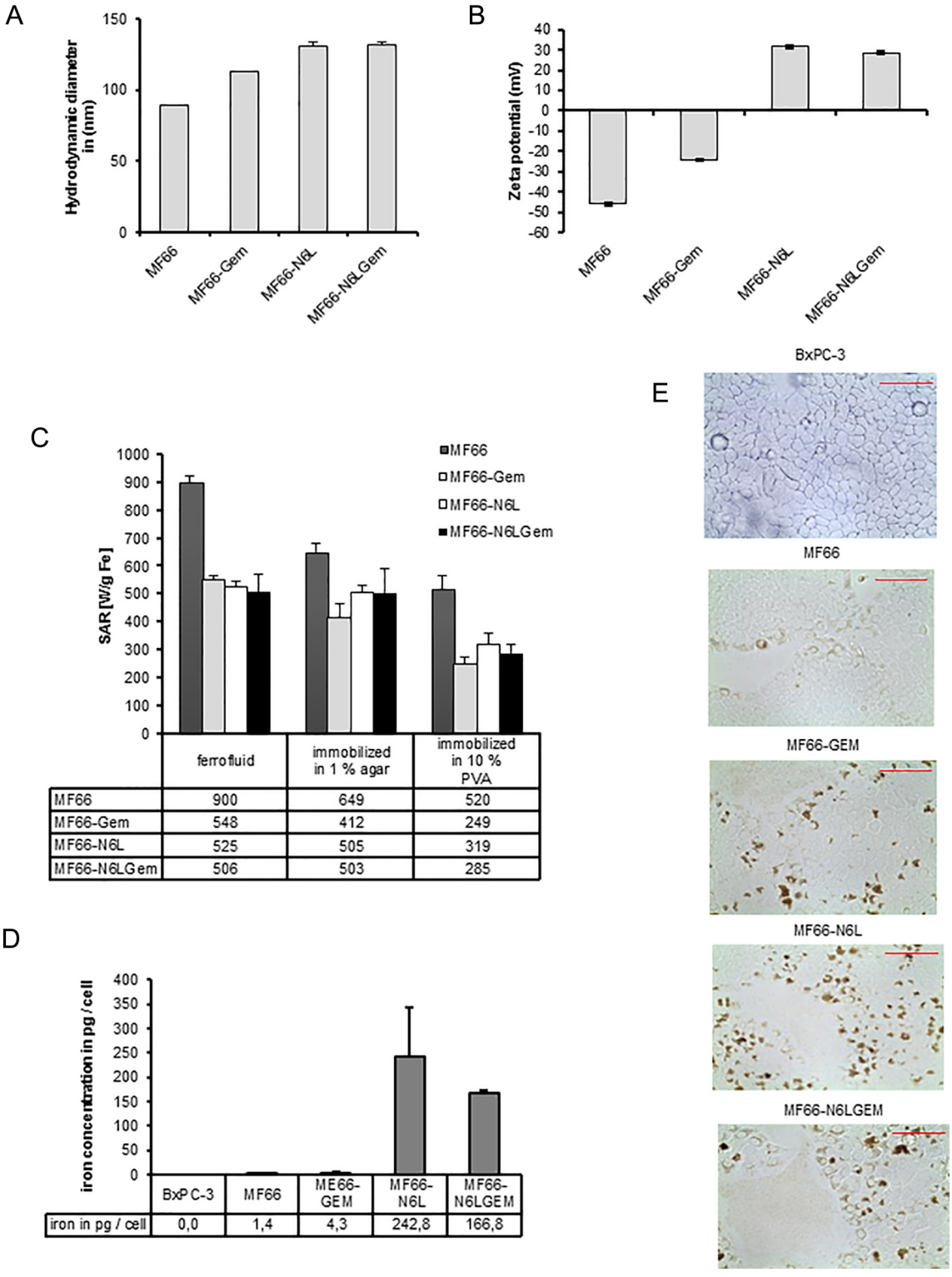

Figure 1. **Characterization of the magnetic nanoparticles (MNP) and their uptake *in vitro*. (A)** The hydrodynamic diameter (z-average); **(B)** the ζ-potential. **(C)** SAR values of MNP. **(D)** Intracellular iron content measured in BxPC-3 24 h following exposure to 100 μg/ml MNP. **(E)** MNP uptake in cells at 24 h after MNP exposure. Scale bar: 100 μm.

Maximal response from Gemcitabine was achieved at 800 μM in either free formulation or conjugated form. The maximal effect was achieved for the conjugated nanoparticle, in the absence of hyperthermia, after 72 h exposure. Nonetheless, cell count reduction and cell permeability are showing cell growth inhibition after 24 h exposure, as reported in Table 1.

Table 1
Comparative cytotoxicity of BxPC-3 cells after exposure with Gemcitabine (Gem), MF-66 conjugated with Gem, MF66 nanoparticles, MF66 conjugated with N6L and Gem and CdSe Quantum dots (Positive control) to pancreatic cells.

	Cell Count reduction[a] [%]		Lysosomal Mass / pH[a] [%]		Cell Permeability[a] [%]	
	24 h	72 h	24 h	72 h	24 h	72 h
Gem (800 μM)	−51	−91	+10	+53	+30	>200
MF66-Gem (100 μg/ml + 800 μM)	−29	−72	+17	+63	>250	170
MF66 MNP (100 μg/ml)	−13	−37	+24	+26	+29	+19
MF66 N6L-Gem (100 μg/ml + 800 μM)	−30	−39	+28	+27	+25	+19
CdSe quantum dots (1 μM)	>−75	>−90	+57	>+80	+95	+135

Data are reported as percentage variation compared to untreated control. (n_{expt} = 3).
[a] Data normalized to untreated control.

The combination of conjugated MNPs and magnetic hyperthermia inhibits cellular growth

Hyperthermia and conjugated MNP exposure (multimodal approach) revealed a prominent inhibition of BxPC-3 and PANC-1 cell growth in comparison to the mono-modal treatment (Figure 2, and Suppl. Figure S1). This holds true for the short-term post incubation times (BxPC-3: 24 to 48 h, Figure 2, *A-C*) as well as for the long term incubation times (15 days, Figure 2, *D-E* and Suppl. Figure S1).

MF66-Gem and MF66-N6LGem induce S-phase cell cycle arrest and increase the sub-G1 fraction irrespectively of magnetic hyperthermia

A prominent increase in S-phase cell fraction was transiently observed for the conjugated MNP formulations (24 h, Figure 3, *A*). Among them, the Gem loaded MNPs displayed a strongest increase in the S-phase cell fraction (BxPC-3, Figure 3, *A*, *C*). Upon subjecting cells to magnetic hyperthermia, this arrest was still detected in cells treated with MF66-Gem and with MF66-N6LGem (Figure 3, *B*, *D*). Native or conjugated MNPs were able to induce apoptosis at short post treatment times (24 h, sub-G1 cell fraction as marker for cell fraction in apoptosis, Figure 3, *E*, and Suppl. Figure S2 for PANC-1cells). At longer post-treatment times (BxPC-3: 48 h), apoptosis was particularly observed for the combination MF66-Gem and MF66-N6LGem and magnetic hyperthermia relative to controls (native cells, MNPs only, Figure 3, *F*). Cell death was also observed in PANC-1 (Suppl. Figure S3) in relation to this therapeutic modality and in certain cases a distinct extent of necrotic cells (Suppl. Figure S3).

Magnetic hyperthermia sensitizes pancreatic tumor cells to gemcitabine therapy and fosters cell death

In both cell lines (PANC-1 and BxPC-3), the highest induction of cell death was registered after treating cells with MNPs conjugated with Gem (compared to non-treated control cells, Figure 4, *A* and *B*, Suppl. Figure S3). This was concomitant to a strong decrease of living cells (Figure 4, *A-D*). Interestingly, subjecting cells to magnetic hyperthermia mostly intensified the effect of Gem on MNPs (either in the mono- or the bi-conjugation mode) in inducing cell death (*i.e.* apoptosis in BxPC-3, Figure 4, *F-H*, but also cell death in PANC-1 cells, Suppl. Figure S3). Conjugation with N6L led to increased cell death and apoptosis compared to the bare MNPs in BxPC-3 and PANC-1 cells. Interestingly, the combinatorial effect of N6L and GEM was not additive (in presence or absence of magnetic hyperthermia, Figure 4, Suppl. Figure S3).

The combination therapy gemcitabine conjugated MNP and magnetic hyperthermia increases intracellular ROS in BxPC-3 cells

The incubation of cells with native or conjugated MNP formulations basically stimulated the production of cellular ROS compared to untreated controls (Figure 5, *A-C*). But after subjecting cells to magnetic hyperthermia, ROS levels distinctly increased in all treatment groups (Figure 5, *A-D*). Cells that have undergone the multi-modal treatment involving Gem conjugated MNP and hyperthermia showed the strongest rise of ROS level compared to the mono-modal treatment with MNPs.

Hyperthermia and the presence of multifunctional MNPs induces cell death by involving apoptotic signaling in the BxPC-3 cells sensitive to gemcitabine

The presence of Gem in the MNP formulations (MF66-Gem, MF66-N6LGem, without hyperthermia) induced an S-phase arrest in cells (Cyclin A, Figure 6, *A* and *D*, lanes 3, 5, 7, 9). DNA damage was confirmed by the increase in protein levels of H2AX (pSer 139) (Figure 6, *A* and *D* lanes 3 and 5). Interestingly, subjecting cells to hyperthermia showed an even stronger increase of H2AX (pSer 139; Figure 6, *A* and *D*, lanes 7-9). Treating cells with the conjugated MNPs and hyperthermia triggered an up-regulation of p53, as well as its downstream target cyclin dependent kinase inhibitor 1A (p21) (Figure 6, *A*, 48 h post treatment). Only the gemcitabine conjugated MNPs and independently form hyperthermia, displayed an increase in p53 and p21 relative to controls, which suggests a persistent stress (Figure 6, *D*, 48 h). The multi-modal treatment (MNPs and hyperthermia) led to an important accumulation of the pro-apoptotic Bax and to a strong reduction of the anti-apoptotic Bcl2 in relation to control group or to MNP treatment. (Figure 6, *D*, lanes 7-9). Besides, we observed a strong activation of caspase-3, caspase-8 (extrinsic apoptotic signaling), and an increase of the cleaved product of PARP (Figure 6, *A-F*). Measurements of caspase-8 activation showed a general increase after incubation with the conjugated MNP in presence of magnetic hyperthermia, particularly with Gem compared to untreated BxPC-3 control cells (Figure 6, *C* and *F*).

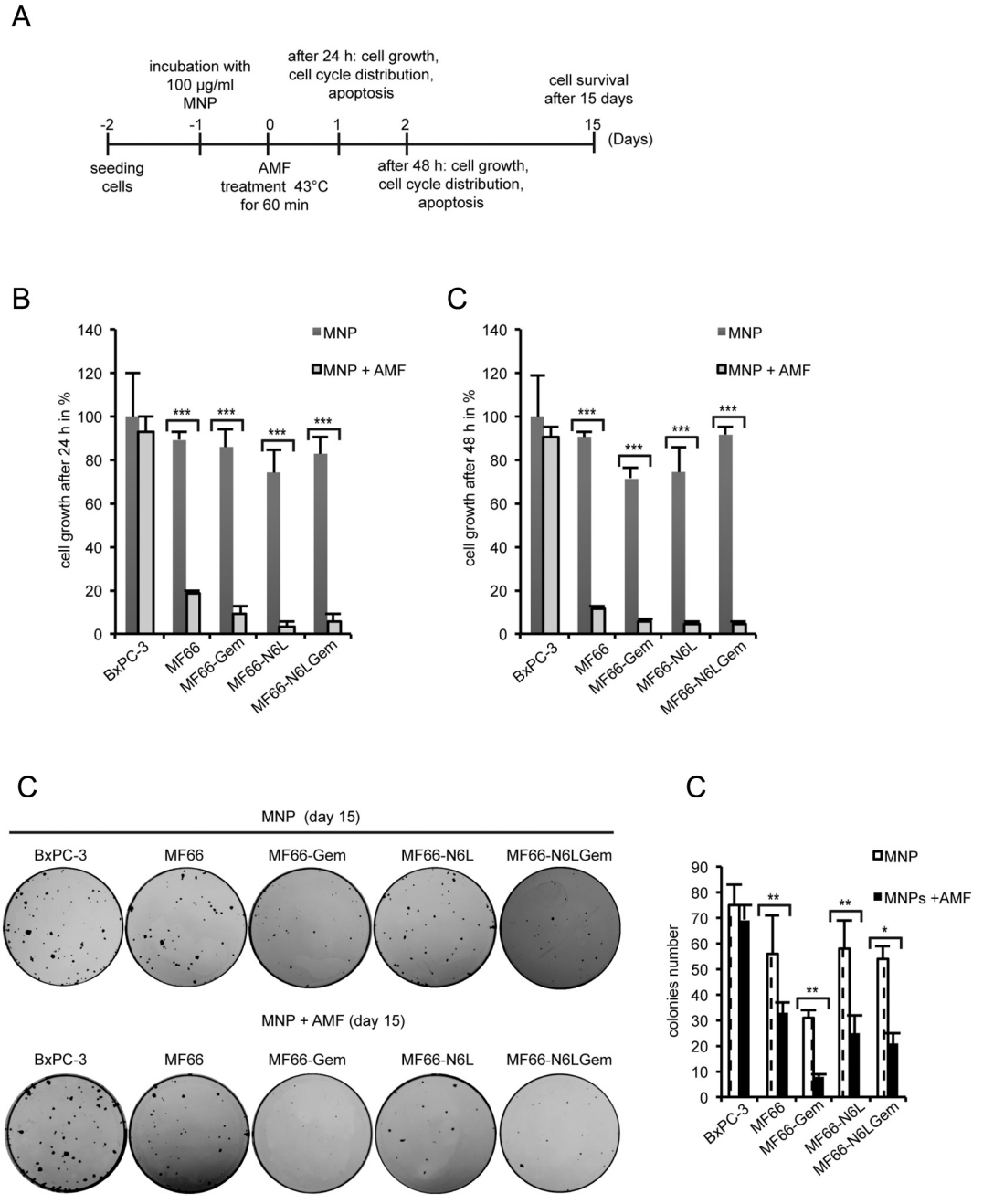

Figure 2. **Magnetic hyperthermia enhances the cytotoxic effect of the conjugated MNP and leads to a strong growth inhibition in BxPC-3 cells *in vitro*. (A)** Working schedule for *in vitro* assays. **(B, C)** Cell growth after treatments (AMF: alternating magnetic field). **(D)** Number of 2D colonies after treatments. **(E)** 15 days post hyperthermia treatment, mean colonies number ± SD. ** $P \leq 0.01$, * $P \leq 0.05$ (n = 3 independent experiments).

Hyperthermia and the presence of multifunctional MNPs induces cell death by a non-apoptosis pathway in the more resistant PANC-1 cells against gemcitabine

In the PANC-1cells, the increase of the pro-apoptotic markers p53, p21, and PARP was less pronounced compared to the gemcitabine sensitive BxPC-3 cells in presence of MF66-Gem or MF66-N6L-Gem, whereas the pro-apoptotic protein Bax remained almost constant (Suppl. Figure S4). Interestingly, the activity of caspase 3/7 was steadily increasing in the presence of MF66-Gem or MF66-N6L-Gem, but in combination with magnetic hyperthermia only prominent at 48 h post treatment (Figure S4).

Hyperthermia in combination with the conjugated MNPs activates the c-Jun N-terminal kinase (JNK) in the sensitive BxPC-3 cells but not in the more resistant PANC-1 cells

In BxPC-3 cells, we could see a decrease of phosphorylated ERK 1/2 (Figure 6, *A*, *D*) in presence of hyperthermia in combination with the conjugated MNPs compared to non-treated

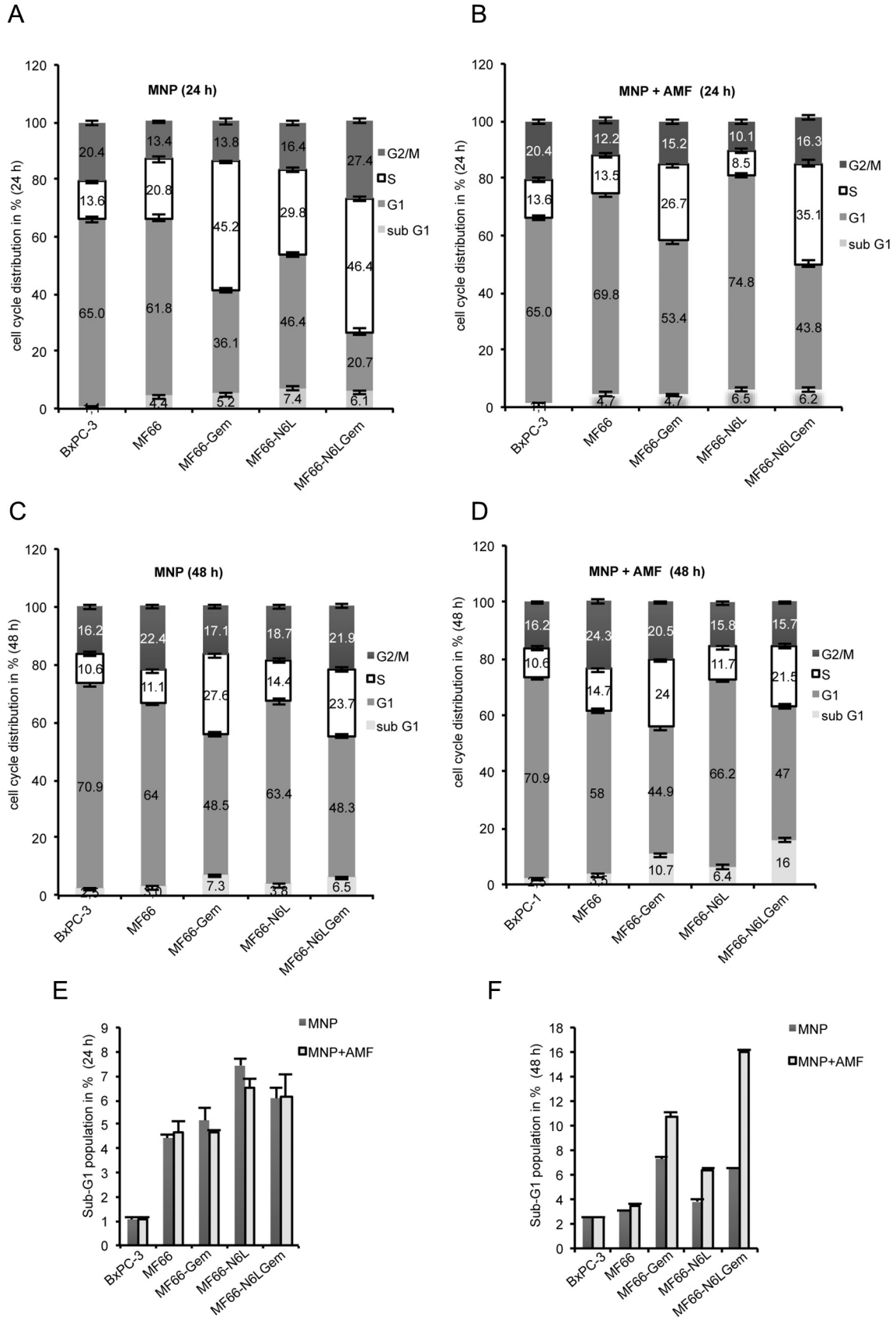

Figure 3. **Treatment of BxPC-3 cells with MF66-Gem and MF66-N6LGem causes an S-phase arrest and sensitize cell killing by the following magnetic hyperthermia**. Cell cycle phase distribution. Mean ± SD (n = 3 independent experiments).

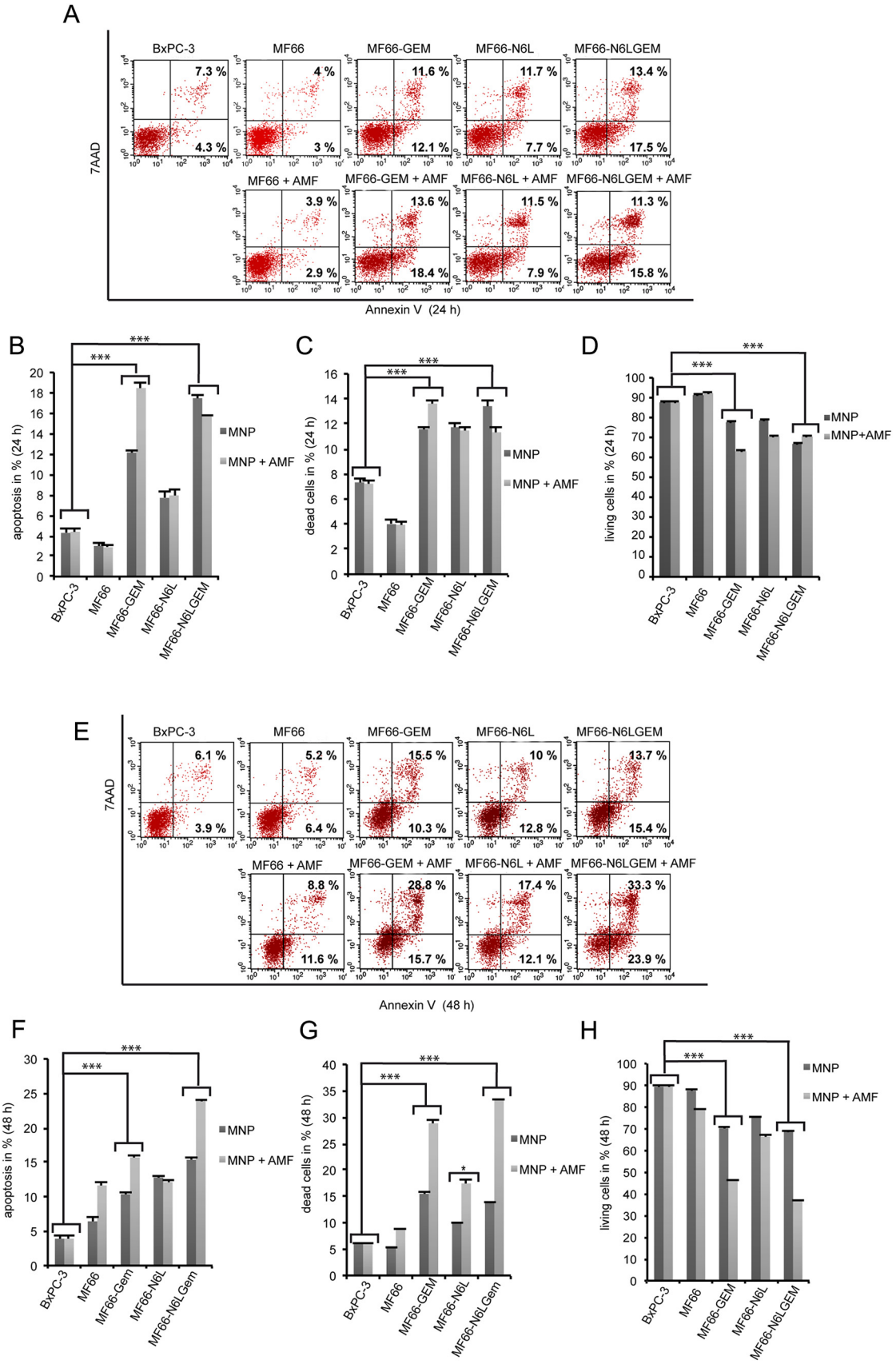

Figure 4. **Magnetic hyperthermia increases apoptosis in BxPC-3 cells pre-treated with MF66-Gem and MF66-N6LGem**. Percentages of apoptotic and death cells; **(D**, **H)** living cells in % (derived from **A** or **E**). Mean ± SD (n = 3 experiments). *** $P \leq 0.001$.

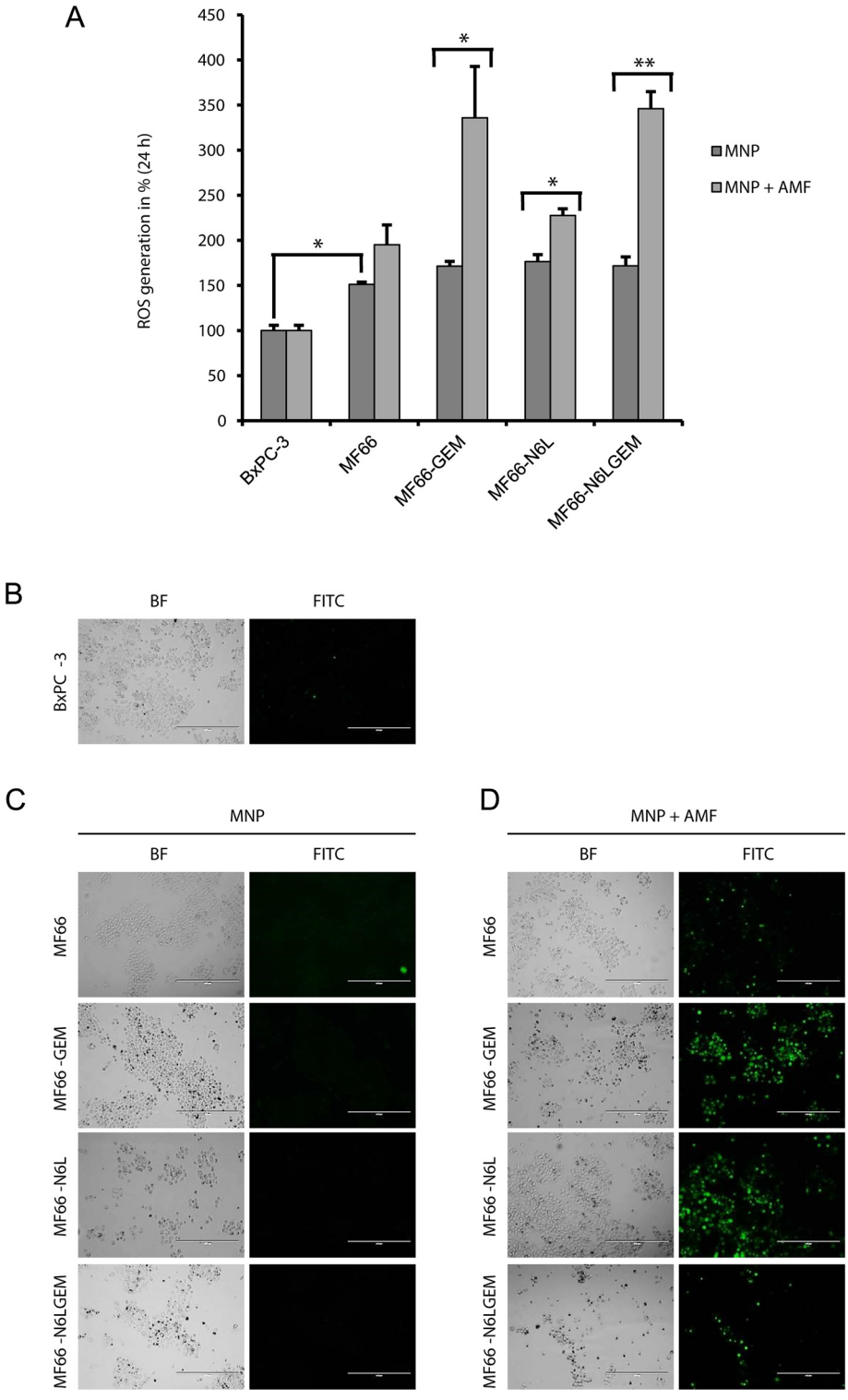

Figure 5. **The combined exposure of** BxPC-3 **cells to MNPs and magnetic hyperthermia enhances the production of intracellular ROS**. **(A)** Intracellular ROS. **(B-D)** Light (BF: bright field) and fluorescence images of intracellular ROS generation. Mean ± SD (n = 3 experiments). * $P \leq 0.05$,** $P \leq 0.01$. Scale bar: 400 μm.

controls. On the other hand, combining Gem conjugated MNP with hyperthermia markedly increased the phosphorylated levels of JNK (Figure 6, *A*, *D*). The overall expression of both kinases, ERK and JNK, remained unchanged (Figure 6, *A*, *D*). In PANC-1 cells, phosphorylated ERK 1/2 was rather increased in presence of hyperthermia in combination with the conjugated MNPs, suggesting resistance. Additionally, phosphorylated levels of JNK were also increased (Suppl. Figure S4).

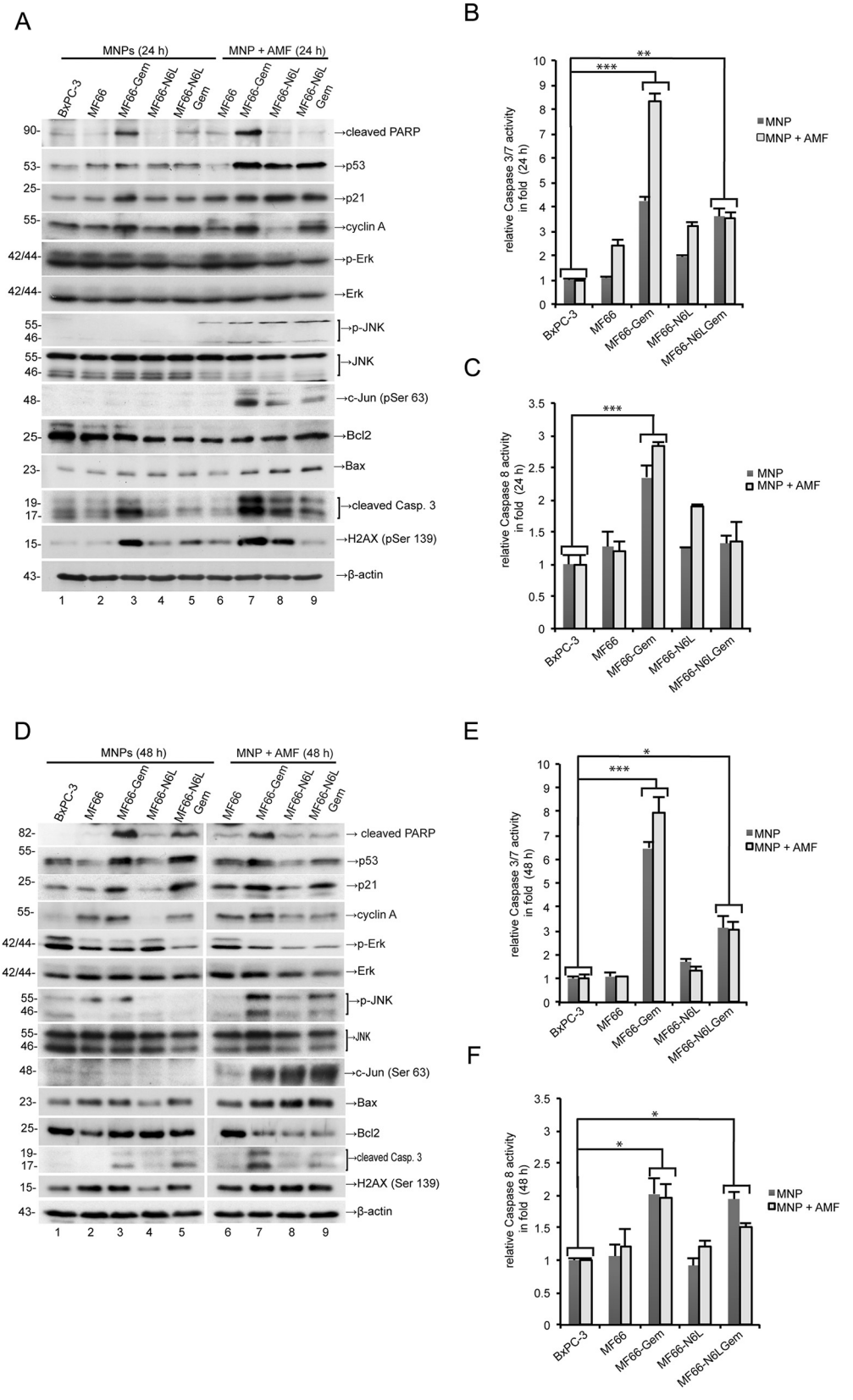

Figure 6. **The treatment with chemotherapeutics coupled to MNP and magnetic hyperthermia activates JNK kinase and triggers more apoptosis in BxPC-3 cells**. **(A, D)** Western Blot analysis of isolated cells. **(B, E)** Activities of caspase 3/7, mean ± SD (n = 3 independent experiments). * $P \leq 0.05$ MNP group *versus* MNP + AMF group, ** $P \leq 0.01$ MNP group *versus* MNP + AMF group. **(C, F)** Activity of caspase 8, mean ± SD (n = 3 independent experiments). * $P \leq 0.05$, ** $P \leq 0.01$, *** $P \leq 0.001$.

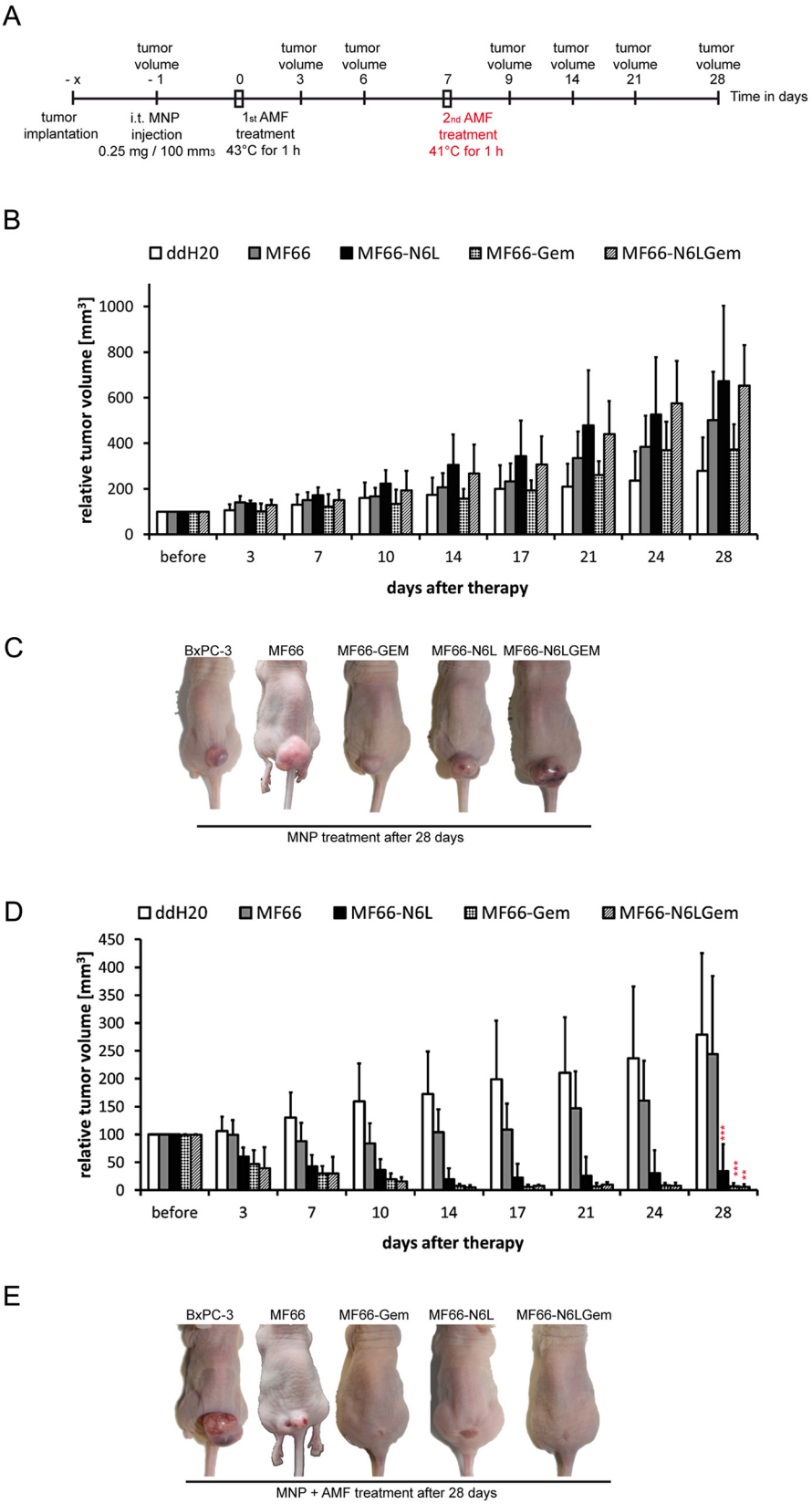

Figure 7. **Combining MNP and magnetic hyperthermia significantly reduces tumor volumes *in vivo*. (A)** Working schedule for magnetic hyperthermia *in vivo*. **(B, D)** Relative tumor volumes to day 0, in %, mean ± SD (n = 8 mice per group). **(C, E)** Macroscopic images (28 days post therapy).**(B, C)** With and **(D, E)** without hyperthermia. *** $P \leq 0.001$ control BxPC-3 *versus* Gem and N6L conjugated MNP and hyperthermia groups. ** $P \leq 0.01$ bare MF66 and hyperthermia *versus* Gem and N6L conjugated MNP and hyperthermia groups.

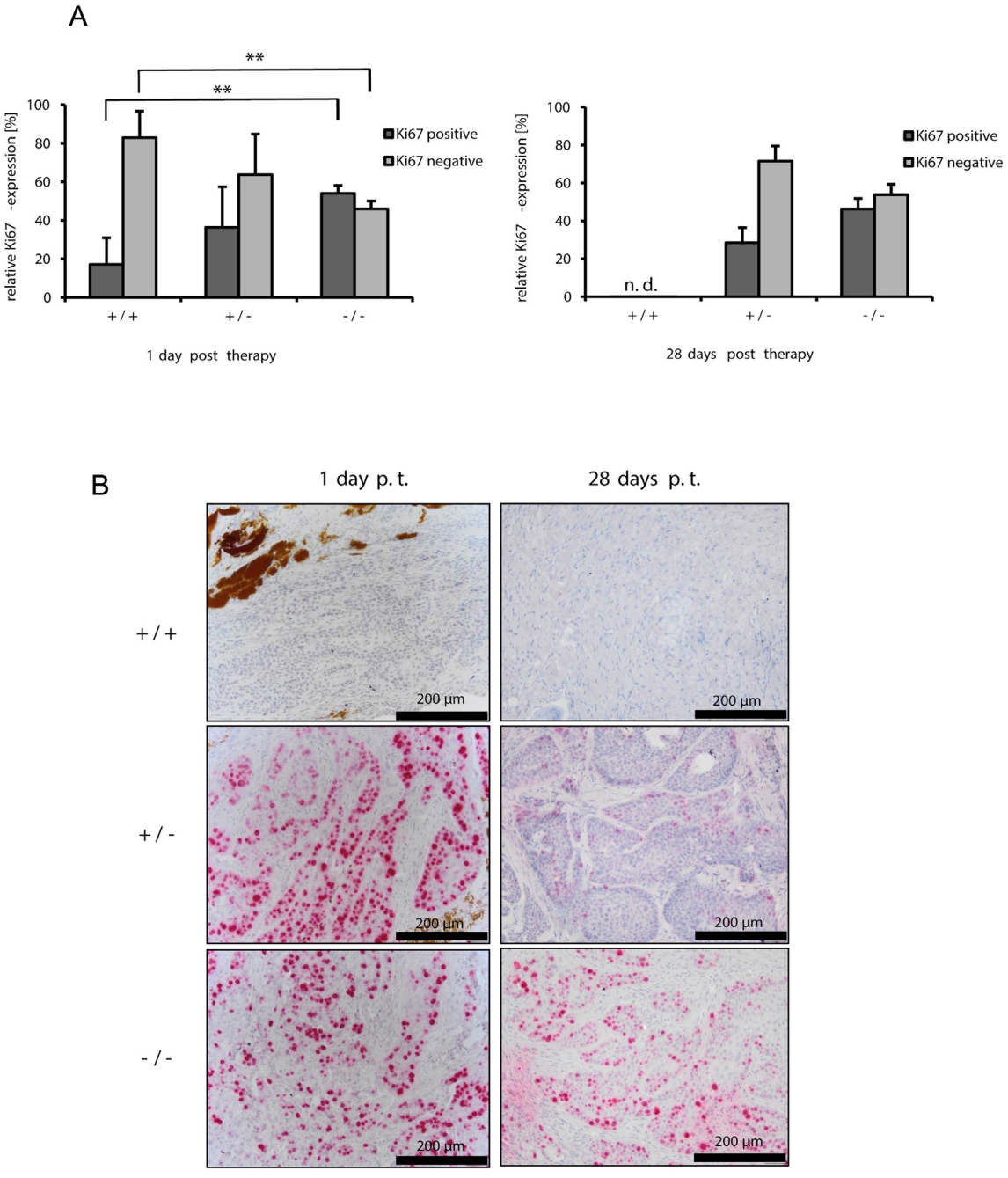

Figure 8. **Combining MF66-N6LGem-MNPs and magnetic hyperthermia distinctly reduces expression of the proliferation marker Ki67 *in vivo*. (A)** Number of Ki67 positive and negative tumor cells in tumor tissue slices. n.d., not determined. **(B)** Exemplary microscopic images, red: Ki67, brown: iron oxide nanoparticles. Bars: 200 µm. +/+: with MNP and AMF; +/−: with MNP and without AMF; −/−: without MNP and without AMF, ** $P \leq 0.01$.

Combining chemotherapeutics conjugated MNP with hyperthermia causes tumor regression in BxPC-3 xenograft model

In absence of hyperthermia all MNP formulations showed a rapid and continuous tumor growth (Figure 7, *A*). The different MNP formulations were not able to reduce tumor volumes compared to control mice (ddH_2O) (Figure 7, *B* and *C*). By contrast, magnetic hyperthermia combined to chemotherapeutics conjugated MNPs showed an impressive tumor regression compared to the initial volume measured at beginning of the experiments (Figure 7, *D* and *E*). This regression was already observed 3 days post hyperthermia treatment and was significant compared to control tumors (ddH_2O + AMF) ($P \leq 0.001$) or those treated with bare MNPs and hyperthermia ($P \leq 0.01$) (Figure 7, *D*). At day 28, tumor volumes reduced for mice treated with MF66-Gem, MF66-N6L or MF66-N6LGem and hyperthermia (Figure 7, *D* and *E*). Interestingly, the mice group treated only with hyperthermia (bare MF66 + AMF) showed a

reduced effect on tumor volumes and 10 days after treatment the tumors restarted to grow (Figure 7, *D*). The combined tumor therapy did not induce any changes of the blood parameters of treated animals (Figure S5).

The combination of AMF treatment and MF66-N6LGem MNP showed a reduced proliferation in the BxPC-3 tumors

At both points in time (1 and 28 days post therapy, Figure 8) a reduction of the number of Ki67-positive and an increase of Ki67- negative cells were observed when tumors were treated with MF66-N6LGem in presence of absence of AMF. The combination of MNP and AMF had a higher impact on the reduced Ki67-expression in tumors than the MNPs alone.

Discussion

Our data show that 1) conjugation of MNPs with Gem and/or N6L fosters their internalization into tumor cells, 2) the coupling procedure does not alter the cytotoxic potential of the drugs, in particular of Gem, 3) the exposure of cancer cells to MNP conjugated with Gem and N6L together with magnetic hyperthermia further strengthens the cytotoxic effect in gemcitabine sensitive and less sensitive cells *in vitro*, 4) the observed anti-tumor effects were also visible in the *in vivo* situation.

In terms of the heating potential, all investigated MNP formulations displayed high SAR values, even after immobilization of the MNPs, in comparison to those reported in the literature.[26,37]

Almost all conjugated MNP formulations displayed an important cellular internalization. In this regard, especially the higher uptake of MNPs can be associated with an increased hydrodynamic diameter after conjugation,[38] or either a direct effect of N6L as a targeting agent nucleophosmin and nucleolin,[20,22] or – at least to a lesser extent – to physicochemical features of the nanoparticles.[39] Interestingly, the exposure of cells with MNPs conjugation with N6L had only a minor effect on cell proliferation and led to higher temperatures upon exposure to the magnetic field compared to the bare MNP due to increased intracellular accumulation.

The conjugated MNP alone exhibited a low cytotoxicity but the different MNP formulations a comparatively higher one as a result of the slow and progressive release of the chemotherapeutics Gem and N6L in absence of hyperthermia. The strong inhibition of cell growth resulting from the multi-modal therapy is related to the locally generated heat induced by magnetic hyperthermia, which might accelerate the drug release from the MNPs.[40]

In the gemcitabine sensitive BxPC-3 cells with IC_{50Gem} of 128 mM[27]), the observed S-phase arrest is an initial response to MF66-Gem or MF66-N6L-Gem, which elicits DNA replication damage during S-phase.[41,42] It is already reported in several studies that free Gem induces an S-phase arrest and triggers apoptosis in cancer cells.[42–45] This means that in particular Gem conjugated to MNPs behaves in the same manner as the free compound. The presence of DNA damage has been corroborated by an enhanced expression of cyclin A, as a key regulatory factor critical for the S-phase, the accumulation of H2AX (pS139), and the rise in the sub-G1 fraction. The data suggest that the S-phase arrest observed after treating cells with Gem conjugated MNPs might be the upstream event leading to apoptosis and the subsequent application of hyperthermia inhibits the DNA repair activity and boosts the cytotoxic effect of Gem on cells by enhancing the sensitivity towards this drug. In consequence, the Gem-based S-phase arrest and inhibition of DNA repair activity might well be one reason for the observed synergistic effect.

Furthermore, we could demonstrate that caspase-8 activation is involved in cell death after treatment with MNPs (MF66-Gem or MF66-N6L-Gem) and hyperthermia. The apoptotic signaling mostly underlies the control of the caspase family. These caspases undergo a sequence of activation steps, which ultimately lead to the induction of apoptosis through cleavage of several substrates.[46] In the gemcitabine sensitive BxPC-3 cells, the combination of hyperthermia and the exposure with conjugated MNPs was able to induce cell death *via* apoptosis (as seen by the modified expression of p53, p21, BcL-2, PARP, Bax, H2AX, S-phase arrest, number of apoptotic cells, *etc.*), either by utilization of the intrinsic or the extrinsic (caspase-8 activation) way. Gem conjugated MNPs in a concentration of 12 μmol GEM/g Fe were still able to activate caspases and induce cell death in absence of hyperthermia. Therefore, Gem-conjugated MNPs and hyperthermia induce apoptosis in Gem sensitive pancreatic BxPC-3 cells mediated by either the intrinsic and extrinsic signaling pathways.

With regard to PANC-1 cells, which are comparatively resistant to Gem (IC_{50Gem} = 300 mM[27]), the increased expression of pro-apoptotic proteins (p53, p21, PARP *etc.*) was less prominent after exposure to magnetic hyperthermia and the conjugated MNPs (MF66-Gem or MF66-N6L-Gem). Nevertheless, this combinatorial therapy still induced a distinct S-phase arrest, an increase of subG1 fraction, a higher number of death cells compared to non-treated controls, *etc.* Interestingly, caspase-3 and caspase-8 were also shown to be involved in PANC-1cell death. Interestingly, caspase-3 and caspase-8 have been shown to mediate cross-talks between programmed cell death (apoptosis) and other cell death mechanisms.[47] Therefore, cells more resistant to the combined therapy may start an interplay among different mechanisms of cell death (*e.g.* autophagy, necroptosis, *etc.*[48]). These findings imply that the higher resistance of these cells might well trigger the induction delayed cell death *via* mechanisms other than classically apoptotic ones.

Beyond the differential sensitivity of BxPC-3 and PANC-1 to Gem, the different effects of the combinatorial therapy on these cells can be attributed to the ability to produce ROS.[49] Namely, hyperthermia is an important trigger of cellular ROS (our data and[50,51]), whereas the sole exposure of cells to the conjugated MNPs (absence of hyperthermia) has a comparatively lower impact on ROS (our own data). When comparing the ability of ROS production among BxPC-3 and PANC-1 after hyperthermia, BxPC-3 cells were more efficient.[28] Subsequently, the differential production of ROS in both cell lines has an impact on the activation of stress responsive kinases. Hereto, in BxPC-3 a sustained activation of JNK (the phosphorylated form p-JNK[52,53]) was found, and to a lesser extent in PANC-1. Interestingly, activated JNK has been linked with apoptosis after Gem treatment (free molecules).[54] Additionally in BxPC-3 cells, we found a substantially reduced level of phosphorylated ERK 1/2, which is an indication of lowered Gem resistance. In contrast in PANC-1 cells, resistance against Gem was increased

(increased activation of ERK 1/2). This increased resistance allows cells to enter at the interplay between cell death and autophagy or other cell death mechanisms.[55]

In vivo Gem-MNPs and hyperthermia therapy achieved almost a complete tumor remission of BxPC-3 in mice xenografts at the end of the experiment (at day 28) in contrast to the groups receiving only the mono-modal MNP therapy, or even hyperthermia alone. In particular, the presence of native or conjugated MNPs seemed to increase tumor growth in this model. One reason might well reside in the responsiveness of the respective tumor cells against oxidative stress. Such relationships were shown to be complex.[56] In contrast the effect was distinctly omitted in presence of hyperthermia. The finding strongly underlines that the combinatorial therapy is compatible to living organisms.

The *in vivo* experiments were done on the base of the intratumoral application of magnetic nanoparticles for hyperthermia treatment. Therefore magnetic hyperthermia might be applicable intraoperatively into pancreatic tumors or, in case the tumor is not totally resectable, by exploiting the present strategies for needle biopsy of pancreatic tumors (*e.g.*[57]). The slow release of the MNPs from the tumor sites permits repeating the hyperthermia treatments.[58] The presence of N6L could foster internalization into tumor cells and the production of lethal intracellular heating spots. The presence of Gem conjugated MNPs might overcome barriers to chemotherapy penetration as a consequence of desmoplastic reactions found in most pancreatic cancers. In this context, we have shown that the concentrations of Gem-coupled to MNP which were utilized to achieve the distinct antitumor effects were of 4.2×10^5 times lower than those commonly used after systemic application in conventional oncology (see supplemental text). Finally, the suggested method is translatable to the clinical situation since both chemotherapeutics Gem[59,60] and N6L (IPP-204106) are established in the clinic and already used in clinical trials and MNPs.

Based on the results of this study, owing to the dual abilities of these MNPs as drug carrier and source of hyperthermia, our conjugated MNPs might be important tools in modeling the efficiency of ROS responsiveness in distinct pancreatic tumor cell phenotypes and therefore foster the induction of cell death in those cells. This would be of great significance in distinctly optimizing local pancreatic tumor treatments.

Appendix A. Supplementary data

Supplementary data to this article can be found online at https://doi.org/10.1016/j.nano.2018.12.019.

References

1. Jemal A, Siegel R, Xu J, Ward E. Cancer statistics. *CA Cancer J Clin* 2010;**60**:277-300.
2. Valetti S, Maione F, Mura S, Stella B, Desmaele D, Noiray M, et al. Peptide-functionalized nanoparticles for selective targeting of pancreatic tumor. *J Control Release* 2014;**192**:29-39.
3. Aires A, Cadenas JF, Guantes R, Cortajarena AL. An experimental and computational framework for engineering multifunctional nanoparticles: designing selective anticancer therapies. *Nanoscale* 2017;**9**:13760-71.
4. Ahmed K, Zaidi SF. Treating cancer with heat: hyperthermia as promising strategy to enhance apoptosis. *J Pak Med Assoc* 2013;**63**:504-8.
5. Shah BP, Pasquale N, De G, Tan T, Ma J, Lee KB. Core-shell nanoparticle-based peptide therapeutics and combined hyperthermia for enhanced cancer cell apoptosis. *ACS Nano* 2014;**8**:9379-87.
6. Ahmed M, Douek M. The role of magnetic nanoparticles in the localization and treatment of breast cancer. *Biomed Res Int* 2013;**2013**281230.
7. Kohler N, Sun C, Wang J, Zhang M. Methotrexate-modified superparamagnetic nanoparticles and their intracellular uptake into human cancer cells. *Langmuir* 2005;**21**:8858-64.
8. Jain TK, Morales MA, Sahoo SK, Leslie-Pelecky DL, Labhasetwar V. Iron oxide nanoparticles for sustained delivery of anticancer agents. *Mol Pharm* 2005;**2**:194-205.
9. Gautier J, Munnier E, Paillard A, Herve K, Douziech-Eyrolles L, Souce M, et al. A pharmaceutical study of doxorubicin-loaded PEGylated nanoparticles for magnetic drug targeting. *Int J Pharm* 2012;**423**:16-25.
10. Alvarez-Berrios MP, Castillo A, Rinaldi C, Torres-Lugo M. Magnetic fluid hyperthermia enhances cytotoxicity of bortezomib in sensitive and resistant cancer cell lines. *Int J Nanomedicine* 2014;**9**:145-53.
11. Sadighian S, Rostamizadeh K, Hosseini-Monfared H, Hamidi M. Doxorubicin-conjugated core-shell magnetite nanoparticles as dual-targeting carriers for anticancer drug delivery. *Colloids Surf B: Biointerfaces* 2014;**117**:406-13.
12. Qu Y, Li J, Ren J, Leng J, Lin C, Shi D. Enhanced magnetic fluid hyperthermia by micellar magnetic nanoclusters composed of Mn(x)Zn (1-x)Fe(2)O(4) nanoparticles for induced tumor cell apoptosis. *ACS Appl Mater Interfaces* 2014;**6**:16867-79.
13. de Sousa Cavalcante L, Monteiro G. Gemcitabine: metabolism and molecular mechanisms of action, sensitivity and chemoresistance in pancreatic cancer. *Eur J Pharmacol* 2014;**741**:8-16.
14. Hui YF, Reitz J. Gemcitabine: a cytidine analogue active against solid tumors. *Am J Health Syst Pharm* 1997;**54**:162-70 [quiz 197-8].
15. Toschi L, Finocchiaro G, Bartolini S, Gioia V, Cappuzzo F. Role of gemcitabine in cancer therapy. *Future Oncol* 2005;**1**:7-17.
16. Baron B, Wang Y, Maehara S, Maehara Y, Kuramitsu Y, Nakamura K. Resistance to gemcitabine in the pancreatic cancer cell line KLM1-R reversed by metformin action. *Anticancer Res* 2015;**35**:1941-9.
17. Hung SW, Marrache S, Cummins S, Bhutia YD, Mody H, Hooks SB, et al. Defective hCNT1 transport contributes to gemcitabine chemoresistance in ovarian cancer subtypes: overcoming transport defects using a nanoparticle approach. *Cancer Lett* 2015;**359**:233-40.
18. Kuramitsu Y, Wang Y, Taba K, Suenaga S, Ryozawa S, Kaino S, et al. Heat-shock protein 27 plays the key role in gemcitabine-resistance of pancreatic cancer cells. *Anticancer Res* 2012;**32**:2295-9.
19. Hilger I. In vivo applications of magnetic nanoparticle hyperthermia. *Int J Hyperth* 2013;**29**:828-34.
20. Destouches D, Page N, Hamma-Kourbali Y, Machi V, Chaloin O, Frechault S, et al. A simple approach to cancer therapy afforded by multivalent pseudopeptides that target cell-surface nucleoproteins. *Cancer Res* 2011;**71**:3296-305.
21. Gilles ME, Maione F, Cossutta M, Carpentier G, Caruana L, Di Maria S, et al. Nucleolin targeting impairs the progression of pancreatic cancer and promotes the normalization of tumor vasculature. *Cancer Res* 2016;**76**:7181-93.
22. Destouches D, El Khoury D, Hamma-Kourbali Y, Krust B, Albanese P, Katsoris P, et al. Suppression of tumor growth and angiogenesis by a specific antagonist of the cell-surface expressed nucleolin. *PLoS One* 2008;**3**e2518.
23. Sader M, Couleaud P, Carpentier G, Gilles ME, Bousserrhine N, Livet A, et al. Functionalization of iron oxide magnetic nanoparticles with the multivalent pseudopeptide N6l for breast tumor targeting. *Nanomed Nanotechnol* 2015;**6**.
24. Kossatz S, Ludwig R, Dahring H, Ettelt V, Rimkus G, Marciello M, et al. High therapeutic efficiency of magnetic hyperthermia in xenograft

models achieved with moderate temperature dosages in the tumor area. *Pharm Res* 2014;**31**:3274-88.
25. Latorre A, Couleaud P, Aires A, Cortajarena AL, Somoza A. Multifunctionalization of magnetic nanoparticles for controlled drug release: a general approach. *Eur J Med Chem* 2014;**82**:355-62.
26. Ludwig R, Stapf M, Dutz S, Muller R, Teichgraber U, Hilger I. Structural properties of magnetic nanoparticles determine their heating behavior - an estimation of the in vivo heating potential. *Nanoscale Res Lett* 2014;**9**:602.
27. Fryer RA, Barlett B, Galustian C, Dalgleish AG. Mechanisms underlying gemcitabine resistance in pancreatic cancer and sensitisation by the iMiD (TM) lenalidomide. *Anticancer Res* 2011;**31**:3747-56.
28. Ludwig R, Teran FJ, Teichgraeber U, Hilger I. Nanoparticle-based hyperthermia distinctly impacts production of ROS, expression of Ki-67, TOP2A, and TPX2, and induction of apoptosis in pancreatic cancer. *Int J Nanomedicine* 2017;**12**:1009-18.
29. Gonzalez RJ, Tarloff JB. Evaluation of hepatic subcellular fractions for Alamar blue and MTT reductase activity. *Toxicol in Vitro* 2001;**15**:257-9.
30. Kossatz S, Grandke J, Couleaud P, Latorre A, Aires A, Crosbie-Staunton K, et al. Efficient treatment of breast cancer xenografts with multifunctionalized iron oxide nanoparticles combining magnetic hyperthermia and anti-cancer drug delivery. *Breast Cancer Res* 2015;**17**:66.
31. Prina-Mello A, Crosbie-Staunton K, Salas G, del Puerto Morales M, Volkov Y. Multiparametric toxicity evaluation of SPIONs by high content screening technique: identification of biocompatible multifunctional nanoparticles for nanomedicine. *IEEE Trans Magn* 2013;**49**.
32. Prina-Mello A, Mohamed BM, Verma NK, Volkov Y. *Advanced Methodologies and Techniques for Assessing Nanomaterial Toxicity*; 2014.
33. Begg AC, Stewart FA, Vens C. Strategies to improve radiotherapy with targeted drugs. *Nat Rev Cancer* 2011;**11**:239-53.
34. Ritter A, Sanhaji M, Steinhauser K, Roth S, Louwen F, Yuan J. The activity regulation of the mitotic centromere-associated kinesin by Polo-like kinase 1. *Oncotarget* 2015;**6**:6641-55.
35. Vermes I, Haanen C, Steffens-Nakken H, Reutelingsperger C. A novel assay for apoptosis. Flow cytometric detection of phosphatidylserine expression on early apoptotic cells using fluorescein labelled Annexin V. *J Immunol Methods* 1995;**184**:39-51.
36. Sanhaji M, Ritter A, Belsham HR, Friel CT, Roth S, Louwen F, et al. Polo-like kinase 1 regulates the stability of the mitotic centromere-associated kinesin in mitosis. *Oncotarget* 2014;**5**:3130-44.
37. Yoo D, Jeong H, Preihs C, Choi JS, Shin TH, Sessler JL, et al. Double-effector nanoparticles: a synergistic approach to apoptotic hyperthermia. *Angew Chem Int Ed Eng* 2012;**51**:12482-5.
38. Iversen TG, Skotland T, Sandvig K. Endocytosis and intracellular transport of nanoparticles: Present knowledge and need for future studies. *Nano Today* 2011;**6**:176-85.
39. Frohlich E. The role of surface charge in cellular uptake and cytotoxicity of medical nanoparticles. *Int J Nanomedicine* 2012;**7**:5577-91.
40. Kettering M, Zorn H, Bremer-Streck S, Oehring H, Zeisberger M, Bergemann C, et al. Characterization of iron oxide nanoparticles adsorbed with cisplatin for biomedical applications. *Phys Med Biol* 2009;**54**:5109-21.
41. Jones RM, Kotsantis P, Stewart GS, Groth P, Petermann E. BRCA2 and RAD51 promote double-strand break formation and cell death in response to gemcitabine. *Mol Cancer Ther* 2014;**13**:2412-21.
42. Hamed SS, Straubinger RM, Jusko WJ. Pharmacodynamic modeling of cell cycle and apoptotic effects of gemcitabine on pancreatic adenocarcinoma cells. *Cancer Chemother Pharmacol* 2013;**72**:553-63.
43. Bouffard DY, Momparler RL. Comparison of the induction of apoptosis in human leukemic cell lines by 2',2'-difluorodeoxycytidine (gemcitabine) and cytosine arabinoside. *Leuk Res* 1995;**19**:849-56.
44. Pauwels B, Korst AE, Pattyn GG, Lambrechts HA, Van Bockstaele DR, Vermeulen K, et al. Cell cycle effect of gemcitabine and its role in the radiosensitizing mechanism in vitro. *Int J Radiat Oncol Biol Phys* 2003;**57**:1075-83.
45. Tolis C, Peters GJ, Ferreira CG, Pinedo HM, Giaccone G. Cell cycle disturbances and apoptosis induced by topotecan and gemcitabine on human lung cancer cell lines. *Eur J Cancer* 1999;**35**:796-807.
46. Cohen GM. Caspases: the executioners of apoptosis. *Biochem J* 1997;**326**(Pt 1):1-16.
47. Sirois I, Groleau J, Pallet N, Brassard N, Hamelin K, Londono I, et al. Caspase activation regulates the extracellular export of autophagic vacuoles. *Autophagy* 2012;**8**:927-37.
48. Marino G, Niso-Santano M, Baehrecke EH, Kroemer G. Self-consumption: the interplay of autophagy and apoptosis. *Nat Rev Mol Cell Biol* 2014;**15**:81-94.
49. Dewhirst MW, Lee CT, Ashcraft KA. The future of biology in driving the field of hyperthermia. *Int J Hyperth* 2016;**32**:4-13.
50. Flanagan SW, Moseley PL, Buettner GR. Increased flux of free radicals in cells subjected to hyperthermia: detection by electron paramagnetic resonance spin trapping. *FEBS Lett* 1998;**431**:285-6.
51. Venkataraman S, Wagner BA, Jiang X, Wang HP, Schafer FQ, Ritchie JM, et al. Overexpression of manganese superoxide dismutase promotes the survival of prostate cancer cells exposed to hyperthermia. *Free Radic Res* 2004;**38**:1119-32.
52. Shen HM, Liu ZG. JNK signaling pathway is a key modulator in cell death mediated by reactive oxygen and nitrogen species. *Free Radic Biol Med* 2006;**40**:928-39.
53. Kamata H, Honda S, Maeda S, Chang L, Hirata H, Karin M. Reactive oxygen species promote TNFalpha-induced death and sustained JNK activation by inhibiting MAP kinase phosphatases. *Cell* 2005;**120**:649-61.
54. Teraishi F, Zhang L, Guo W, Dong F, Davis JJ, Lin A, et al. Activation of c-Jun NH2-terminal kinase is required for gemcitabine's cytotoxic effect in human lung cancer H1299 cells. *FEBS Lett* 2005;**579**:6681-7.
55. Golstein P, Kroemer G. Cell death by necrosis: towards a molecular definition. *Trends Biochem Sci* 2007;**32**:37-43.
56. Valko M, Rhodes CJ, Moncol J, Izakovic M, Mazur M. Free radicals, metals and antioxidants in oxidative stress-induced cancer. *Chem Biol Interact* 2006;**160**:1-40.
57. Dahring H, Grandke J, Teichgraber U, Hilger I. Improved hyperthermia treatment of tumors under consideration of magnetic nanoparticle distribution using micro-CT imaging. *Mol Imaging Biol* 2015;**17**:763-9.
58. Jeon MJ, Ahn CH, Kim H, Chung IJ, Jung S, Kim YH, et al. The intratumoral administration of ferucarbotran conjugated with doxorubicin improved therapeutic effect by magnetic hyperthermia combined with pharmacotherapy in a hepatocellular carcinoma model. *J Exp Clin Cancer Res* 2014;**33**:57.
59. Lee MY, Jung KS, Kim HS, Lee JY, Lim SH, Kim M, et al. Weekly docetaxel and gemcitabine in previously treated metastatic esophageal squamous cell carcinoma. *World J Gastroenterol* 2015;**21**:4268-74.
60. Van Zweeden A, van der Vliet H, Wilmink J, Meijerink M, Meijer O, Bruynzeel A, et al. Phase I clinical trial to determine the feasibility and maximum tolerated dose of panitumumab to standard gemcitabine-based chemoradiation in locally advanced pancreatic cancer. *Clin Cancer Res* 2015;**21**, https://doi.org/10.1158/1078-0432.CCR-14-3364.